

A study of electronic structure of $\text{FeSe}_{1-x}\text{Te}_x$ chalcogenides by Fe and Se K-edge x-ray absorption near edge structure measurements

B. Joseph¹, A. Iadecola¹, L. Simonelli², Y. Mizuguchi^{3,4}, Y. Takano^{3,4}, T. Mizokawa^{5,6}, N. L. Saini^{1,6}

¹Dipartimento di Fisica, Università di Roma “La Sapienza”, P. le Aldo Moro 2, 00185 Roma, Italy

²European Synchrotron Radiation Facility, 6 RUE Jules Horowitz BP 220 38043 Grenoble Cedex 9 France

³National Institute for Materials Science, 1-2-1 Sengen, Tsukuba 305-0047, Japan

⁴JST-TRIP, 1-2-1 Sengen, Tsukuba 305-0047, Japan

⁵Department of Physics, University of Tokyo, 5-1-5 Kashiwanoha, Kashiwa, Chiba 277-8561, Japan

⁶Department of Complexity Science and Engineering, University of Tokyo, 5-1-5 Kashiwanoha, Kashiwa, Chiba 277-8561, Japan

Abstract.

Fe K-edge and Se K-edge x-ray absorption near edge structure (XANES) measurements are used to study $\text{FeSe}_{1-x}\text{Te}_x$ electronic structure of chalcogenides. An intense Fe K-edge pre-edge peak due to Fe $1s \rightarrow 3d$ (and admixed Se/Te p states) is observed, showing substantial change with the Te substitution and X-ray polarization. The main white line peak in the Se K-edge XANES due to Se $1s \rightarrow 4p$ transition appear similar to the one expected for Se^{2-} systems and changes with the Te substitution. Polarization dependence reveals that unoccupied Se orbitals near the Fermi level have predominant $p_{x,y}$ character. The results provide key information on the hybridization of Fe $3d$ and chalcogen p states in the Fe-based chalcogenide superconductors.

PACS numbers: 74.70.Xa;61.05.cj;74.81-g

1. Introduction

Observation of superconductivity in the $\text{FeSe}_{1-x}\text{Te}_x$ chalcogenides with interplaying superconductivity and magnetism [1, 2, 3, 4, 5] is of high interest due to apparent simplicity of these materials in comparison to the Fe-based pnictides [6, 7]. Indeed, the structure of $\text{FeSe}_{1-x}\text{Te}_x$ contains a simple stacking of edge sharing $\text{Fe}(\text{Se},\text{Te})_4$ tetrahedra [1, 2, 3] without any sandwiching spacer [8]. The superconductivity is very sensitive to defects and disorder [9], with the T_c in the ternary $\text{FeSe}_{1-x}\text{Te}_x$ system increasing up to a maximum of 14 K [2, 3, 10]. However, the missing spacer layer in the $\text{FeSe}_{1-x}\text{Te}_x$ might be a cause of locally broken symmetry in the ternary system [11, 12, 13, 14] with the Se and Te occupying distinct sites. Although, the electronic states near the Fermi level in the $\text{FeSe}_{1-x}\text{Te}_x$ chalcogenides are given by the five Fe 3d-orbitals, it is also true that the fundamental transport properties are very sensitive to the chalcogen (Se/Te) height from the Fe-Fe sublattice [15, 16, 17], indicating importance of interaction of Fe 3d states with the chalcogen orbitals. Therefore, it is of key importance to study details on the electronic structure of the Fe 3d and the interacting chalcogen orbitals.

X-ray absorption near-edge structure (XANES) spectroscopy is a site specific probe of distribution of the valence electrons and local chemistry, with the final states in the continuum being due to multiple scattering resonances of the photoelectron in a finite cluster [18]. Unlike photoemission experiments, there are negligible surface effects (and multiplet effects), making it a very useful finger print probe of unoccupied valence states and site selective local chemistry. The XANES spectroscopy has been already used to study the electronic structure and the local geometry in the Fe-based REFeAsO (RE=rare earth) oxypnictides [19, 20, 21, 22, 23, 24, 25, 26] and AFe_2As_2 (A=Ba,Sr,Ca) pnictides [26, 27]. Indeed, important information on the electronic correlations [21, 22, 26] as well on the local geometry [19, 20, 23] has been obtained. However, there is hardly any systematic XANES study on the Fe-based chalcogenides. Here, we have used XANES spectroscopy to study electronic structure of unoccupied states in $\text{FeSe}_{1-x}\text{Te}_x$ system. A combined analysis of Fe and Se K-edge XANES has permitted to uncover important features of the unoccupied states near the Fermi level. We find a substantial hybridization between the Fe 3d and chalcogen p states, getting redistributed systematically with the Te substitution. Furthermore, using polarized XANES on single crystal sample, we have found that chalcogen p_{xy} orbitals should be predominantly interacting with the Fe 3d orbitals in the chalcogenides. The results underline importance of the $p-d$ hybridization in the Fe-based chalcogenide superconductors.

2. Experimental Details

Unpolarized and polarized X-ray absorption measurements were made at the beamline BM29 of the European synchrotron radiation facility (ESRF), Grenoble, on the $\text{FeSe}_{1-x}\text{Te}_x$ samples characterized for their superconducting and structural properties

[28, 29]. Unpolarized spectra were measured on powder samples [28] of $\text{FeSe}_{1-x}\text{Te}_x$ ($x=0.0, 0.5, 1.0$) to explore the composition dependence, while single crystal sample of $\text{FeSe}_{0.25}\text{Te}_{0.75}$ [29] was selected to study polarization dependence of the XANES features. The synchrotron radiation emitted by a bending magnet source at the 6 GeV ESRF storage ring was monochromatized by a double crystal Si(311) monochromator and sagittally focused on the samples, mounted in a continuous flow He cryostat. For the polarized measurements on the $\text{FeSe}_{0.25}\text{Te}_{0.75}$ single crystal sample, normal incidence geometry with linearly polarized light falling parallel to the ab-plane and grazing incidence geometry with linearly polarized light falling nearly perpendicular to the ab-plane were used. The Se K-edge absorption spectra were recorded by detecting the Se K_α fluorescence photons, while Fe K_α fluorescence photons were collected over a large solid angle using multi-element Ge-detector for measuring the Fe K-edge absorption. For the unpolarized spectra on the powder samples we used simultaneous detection of the fluorescence signal and the transmission yield. The sample temperature was controlled and monitored within an accuracy of ± 1 K. As a routine experimental approach, several absorption scans were collected to ensure the reproducibility of the absorption spectra, in addition to the high signal to noise ratio. After subtracting linear pre-edge background, the XANES spectra were normalized to the energy dependent atomic absorption, estimated by a linear fit to the extended x-ray absorption fine structure (EXAFS) region away from the absorption edge.

3. Results and Discussion

3.1. Fe K-edge XANES

Figure 1 shows normalized Fe K-edge XANES spectra of $\text{FeSe}_{1-x}\text{Te}_x$ ($x=0.0, 0.5, 1.0$) measured at $T = 30$ K. The spectra are close to the one for a reference of Fe^{2+} standard [23, 25], consistent with the Fe^{2+} state. The general features of the Fe K-edge are similar to those reported for the Fe-based pnictides [23, 24, 25]. The near edge features are marked with A, B, C, D and E. The K-edge absorption process is mainly governed by the $1s \rightarrow \epsilon p$ dipole transition and hence continuum states with ϵp symmetries (and admixed states) can be reached in the final state. In addition to the dipole transition, a direct quadrupole transition in the unoccupied $3d$ states is seen as pre-peak A, mixed with the dipole contribution (mixing with the $4p$ states due to local distortions). Therefore, apart from the density of the unoccupied electronic states, a changing pre-edge intensity can be an indicator of a changing local geometry or distortion around the Fe atom. Here, the pre-peak A (~ 7111 eV) is due to the $1s \rightarrow 3d$ quadrupole transition, with some dipole contribution due to the admixed p states. The feature B (shoulder structure of the main absorption jump at ~ 7117 eV) appears due to the $1s \rightarrow 4p$ transition. The peak like structure C (~ 7120 eV) should be driven by the $1s \rightarrow 4p$ states admixed with the d states of the chalcogen atoms. A significant change in the pre-peak A intensity can be seen as a function of Te substitution with the one for the FeSe appearing more intense

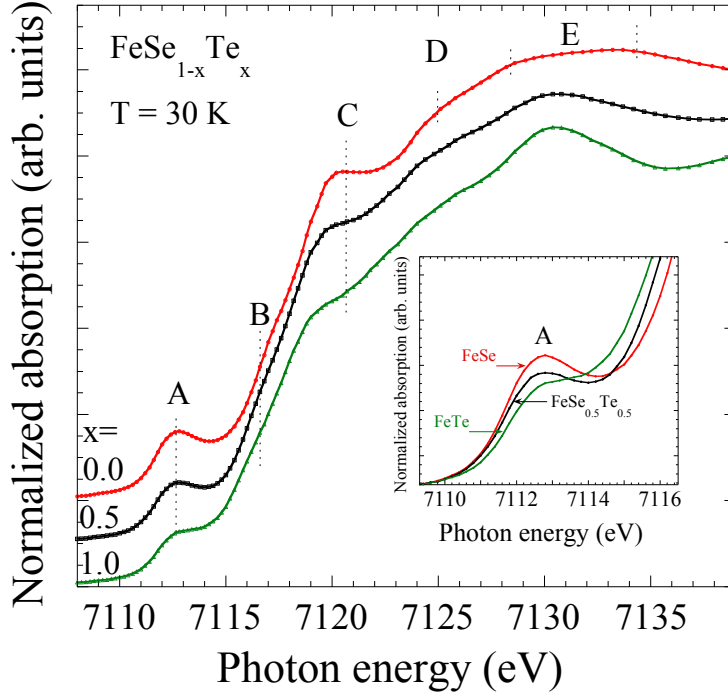


Figure 1. Fe K-edge XANES spectra of $\text{FeSe}_{1-x}\text{Te}_x$ ($x=0, 0.5, 1$) measured at 30 K. The inset shows a zoom over the near edge features A.

(see e.g., the inset showing a zoom over the peak A). Similarly, the feature C looks more intense for the FeSe sample due to larger mixing of Fe 4*p*/chalcogen *d* states. The features at higher energies are mainly due to the photoelectron multiple scattering with the nearest neighbours.

For a further clarification on the Fe K-edge spectral features, we have studied polarization dependence of the XANES measured on a single crystal of representative $\text{FeSe}_{0.25}\text{Te}_{0.75}$ sample. Fig. 2. shows the Fe K-edge XANES spectra with varying polarization. A significant polarization dependence of Fe K-edge features can be seen. In particular, the pre-peak shows a significant increase from parallel to the almost perpendicular polarization ($E||75$ degree). This indicates increased density of unoccupied Fe 3*d* states admixed with the *p* states originated from the chalcogen atoms. The polarization dependence appears similar to the one found for the oxypnictides [25]. The results also appear consistent with the local-density approximation (LDA) calculations for these materials [15]. Similarly, the peak C gets more intense for the perpendicular geometry, mainly due to higher density of states for Fe 4*p*/chalcogen *d* hybrid bands along the *c*-axis. On the other hand, the peak B appears hardly affected with the polarization. The polarization dependence can be understood also in terms of different local geometry of the system in the the two directions. Indeed, with $E||ab$ plane, the Fe-Fe planar orbitals are available for the transition while with $E||c$, the mixing of the chalcogen *p* (peak A) and chalcogen *d* (peak C) is expected to be more

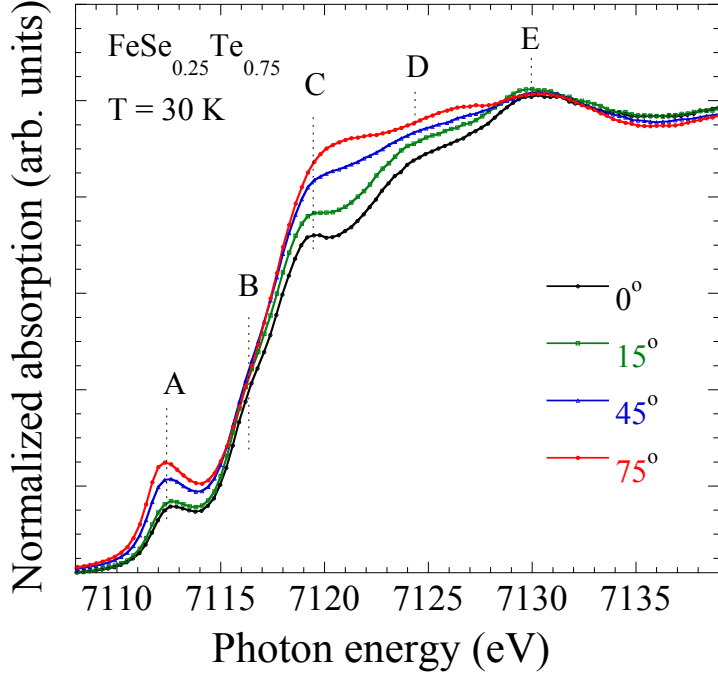


Figure 2. Polarized Fe K-edge XANES spectra of $\text{FeSe}_{0.25}\text{Te}_{0.75}$ measured at 30 K. The 0° correspond to the $E\parallel ab$ while the 75° represent almost $E\parallel c$ case. Strong polarization effect is evident on the pre-peak A and the peak C.

prominent.

Coming back to the substitution effect (Fig. 1), a clear energy shift can be seen for the features B and the peak C. Indeed, the peak C is shifted by almost 0.8 eV lower energy for the FeTe with respect to the FeSe. Since this peak is derived by the Fe-chalcogen orbitals mixing, any change in the Fe-chalcogen bond length is expected to influence the peak position, related by the $\Delta E \propto 1/d^2$ relation for a XANES resonance [30]. The Fe-chalcogen bondlength in the FeTe is $\approx 2.6 \text{ \AA}$, larger than the Fe-chalcogen bondlength in the FeSe ($\approx 2.4 \text{ \AA}$). A gradual and substantial decrease of the pre-peak (Fig. 1) derived by $1s \rightarrow 3d$ quadrupole transition and a dipole transition due to admixed chalcogen p states is consistent with the longer Fe-Te distance. On the other hand, an apparent broadening and the shift of the peak C for the $\text{FeSe}_{0.5}\text{Te}_{0.5}$ should be due to the local inhomogeneity of the ternary system, characterized by coexisting Fe-chalcogen bondlengths [11, 12, 13, 14]. Similarly, the peak B is shifted towards lower energy for the FeTe with respect to the FeSe, merely due to the fact that the Fe-Fe bondlength for the FeSe ($\approx 2.66 \text{ \AA}$) is lower than the one for the FeTe ($\approx 2.69 \text{ \AA}$). Following the above arguments we can state that the higher intensity of the pre-peak should be due to higher mixing of the chalcogen p orbitals with the Fe $3d$ states consistent with the shorter Fe-chalcogen bondlength, and hence the dipole contribution appears to be changing, with higher number of available unoccupied states for the transition from the Fe $1s$ states. It should be mentioned that a sophisticated theoretical model is required

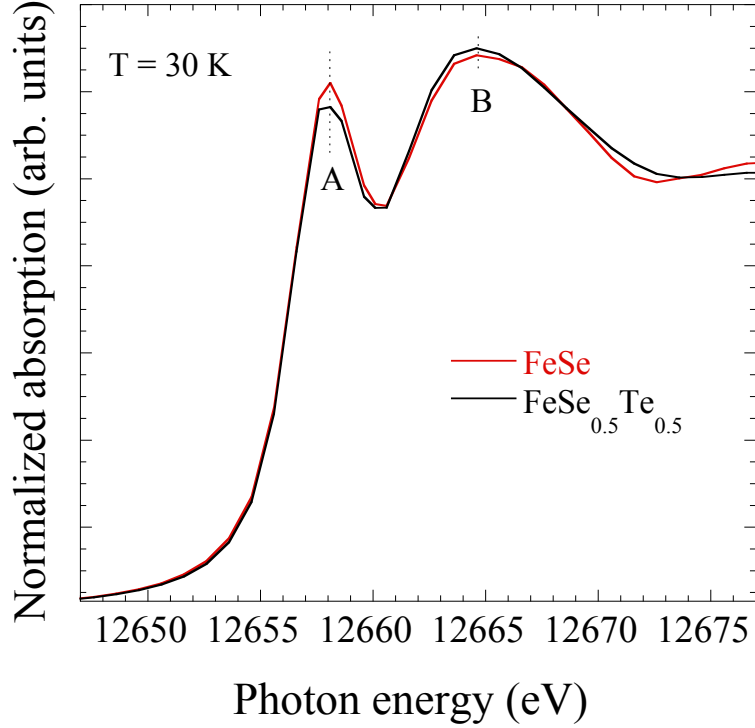


Figure 3. Se K-edge XANES spectra of $\text{FeSe}_{1-x}\text{Te}_x$ ($x=0, 0.5$) measured at $T = 30$ K.

for a quantitative estimation of the dipole and quadrupole contribution in the present system with Fe in a tetrahedral geometry.

3.2. Se K-edge XANES

Figure 3 compares Se K-edge XANES spectra of FeSe and $\text{FeSe}_{0.5}\text{Te}_{0.5}$ samples measured at $T = 30$ K. There are two main features, (i) a sharp peak A (~ 12658 eV), which is mainly due to a direct $1s \rightarrow 4p$ dipole transition and, (ii) the broad hump B (about 7 eV above the peak A), should be a multiple scattering of the photoelectron with the near neighbours. The spectra are typical of Se^{2-} systems [31, 32] with position of the peak A in all the samples being consistent with earlier studies on similar systems. The peak A appears to have lower intensity for the Te substituted samples, suggesting decreased number of unoccupied Se $4p$ states near the Fermi level with Te substitution. In addition, the multiple scattering hump B shows some evident changes with the Te substitution, mainly due to changing local geometry around the Se atoms. Indeed, this hump appears to be getting broader for the Te substituted samples with an overall shift towards lower energy. This should be related to local inhomogeneity of the ternary system, seen by EXAFS measurements [11, 12].

To have further details of the unoccupied Se electronic states, we have measured the Se K-edge XANES in different polarizations on the $\text{FeSe}_{0.25}\text{Te}_{0.75}$ single crystal sample.

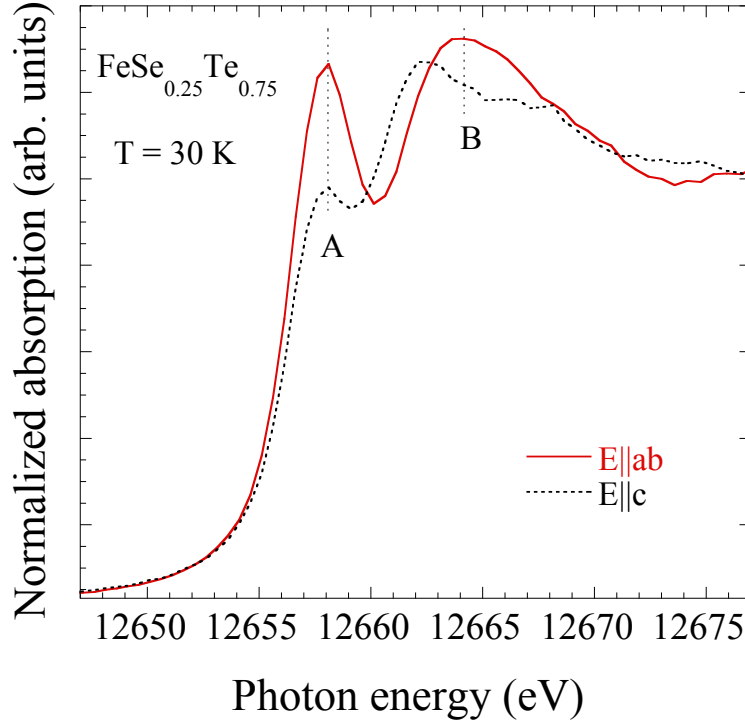


Figure 4. Polarized Se K-edge XANES spectra of $\text{FeSe}_{0.25}\text{Te}_{0.75}$ crystal measured at $T = 30$ K with polarization of the beam along the two high symmetry crystal axes.

Fig. 4 shows normalized Se K-edge XANES measured with the polarization parallel and nearly perpendicular to the ab -plane of the single crystal sample. There is large polarization dependence, with the peak A due to the $1s \rightarrow 4p$ dipole transition appearing extremely damped in the spectrum obtained using perpendicular polarization. This merely brings a conclusion that unoccupied Se $4p$ states near the Fermi level in these systems are mainly derived by the $p_{x,y}$ symmetry. Incidentally, the hump B also shows a strong polarization effect. Indeed, the hump has very different spectral shape in the two geometries, appearing with apparently two broad features in the $E||c$ geometry unlike a single broad feature in the $E||ab$ geometry. The lower energy feature of the hump in the $E||c$ geometry shows an overall shift with respect to the hump in the $E||ab$ geometry. Since the hump is due to multiple scattering including Se-Fe, Se-Se and Se-Te shells, different spectral shapes are likely to be due to different contributions of these scattering paths in the two polarization geometries. The fact that, while Se-Fe paths are equally seen in the two geometries, the Se-Se/Te paths are different with some of the scattering paths missing in the $E||c$ geometry, and hence an apparent two peak spectral shape in the $E||c$ geometry unlike a broader hump B for the $E||ab$ polarization. However, shell by shell full multiple scattering calculations need to be performed to study the details of these local geometrical variations, which are beyond the scope of the present papers focus on the electronic structure.

4. Summary

In summary, we have studied electronic structure of $\text{FeSe}_{1-x}\text{Te}_x$ chalcogenides by a combination of Fe and Se K-edge X-ray absorption near edge structure spectroscopy. From the Fe K-edge data we find a gradual and substantial decrease of the pre-peak derived by $1s \rightarrow 3d$ quadrupole transition and a dipole transition due to admixed chalcogen p states. The damping seems to be due to lower mixing of chalcogen p states in the Te containing systems, consistent with the longer Fe-Te distance. Again, the Se K-edge XANES spectra reveal a damping of unoccupied $4p$ states, consistent with the Fe K-edge XANES suggesting lower admixing of the Fe $3d$ with the chalcogen p states in the Te containing systems. Furthermore, the polarized Se K-edge XANES reveals predominant $p_{x,y}$ character of the chalcogen p states that should be involved in the admixing with the unoccupied Fe $3d$ states near the Fermi level. The results are consistent with strong chalcogen height sensitivity of the fundamental electronic structure, that seems to be related with redistribution of the admixed Fe $3d$ - chalcogen p states.

Acknowledgments

The authors thank the ESRF staff for the help and cooperation during the experimental run.

References

- [1] Hsu, F.-C., Luo, J.-Y., Yeh, K.-W., Chen, T.-K., Huang, T.-W., Wu, P. M., Lee, Y.-C., Huang, Y.-L., Chu, Y.-Y., Yan, D.-C., Wu, M.-K., Proc. Nat. Acad. Sci. 105, 14262 (2008).
- [2] Fang M. H., Pham H. M., Qian B., Liu T. J., Vehstedt E. K., Liu Y., Spinu L., and Mao Z. Q., Phys. Rev. B 78, 224503 (2008).
- [3] Yeh, K.-W., Huang, T.-W., Huang, Y.-l., Chen, T.-K., Hsu, F.-C., Wu, P. M., Lee, Y.-C., Chu, Y.-Y., Chen, C.-L., Luo, J.-Y., Yan, D.-C., Wu, M.-K., EPL 84, 37002 (2008).
- [4] Medvedev, S., McQueen, T. M., Troyan, I. A., Palasyuk, T., Eremets, M. I., Cava, R. J., Naghavi, S., Casper, F., Ksenofontov, V., Wortmann, G., Felser, C., Nat. Mat. 8, 630-633 (2009).
- [5] Khasanov, R., Bendele, M., Amato, A., Babkevich, P., Boothroyd, A. T., Cervellino, A., Conder, K., Gvasaliya, S. N., Keller, H., Klauss, H. H., Luetkens, H., Pomjakushin, V., Pomjakushina, E., Roessli, B., Phys. Rev. B 80, 140511 (2009).
- [6] Ishida K., Nakai Y., and Hosono H., J. Phys. Soc. Jpn. 78, 062001 (2009).
- [7] Ren Z.-A. and Zhao Z.-X., Advanced Materials 21, 4584 (2009), ISSN 1521-4095.
- [8] Ricci A., Joseph B., Poccia N., Xu W., Chen D., Chu W.S., Wu Z.Y., Marcelli A., Saini N.L. and Bianconi A., Supercond. Sci. Technol. 23, 052003 (2010).

- [9] McQueen, T. M., Williams, A. J., Stephens, P. W., Tao, J., Zhu, Y., Ksenofontov, V., Casper, F., Felser, C., Cava, R. J., Phys. Rev. Lett. 103, 057002 (2009);
McQueen T. M., Huang Q., Ksenofontov V., Felser C., Xu Q., Zandbergen H., Hor Y. S., Allred J., Williams A. J., Qu D., Checkelsky J., Ong N. P., Cava R. J., Phys. Rev. B 79, 014522 (2009).
- [10] Horigane, K., Hiraka, H., Ohoyama, K., J. Phys. Soc. Jpn. 78, 074718 (2009).
- [11] Joseph B., Iadecola A., Puri A., Simonelli L., Mizuguchi Y., Takano Y., and Saini N. L., Phys. Rev. B 82, 020502(R) (2010).
- [12] Iadecola A., Joseph B., Simonelli L., Mizuguchi Y., Takano Y. and Saini N. L., EPL, 90, 67008 (2010).
- [13] Louca D., Horigane K., Llobet A., Arita R., Ji S., Katayama N., Konbu S., Nakamura K., Koo T.-Y., Tong P., and Yamada K., Phys. Rev. B 81, 134524 (2010).
- [14] Tegel M., Loehnert C., Johrendt D., Solid State Commun. 150, 383 (2010).
- [15] Miyake, T., Nakamura, K., Arita, R., Imada, M., J. Phys. Soc. Jpn. 79 044705 (2010).
- [16] Moon, C.-Y., Choi, H. J., Phys. Rev. Lett. 104, 057003 (2010).
- [17] Subedi, A., Zhang, L., Singh, D. J., Du, M. H., Phys. Rev. B 78, 134514 (2009).
- [18] Bianconi A., Dell’Ariccia M., Durham P. J. and Pendry J. B., Phys. Rev. B 26, 6502 (1982);
EXAFS and Near Edge Structure edited by Bianconi A., Incoccia L., and Stipcich S. (Springer-Verlag, Berlin, 1982);
Bianconi A. in X-ray Absorption: Principles, Applications, Techniques of EXAFS, SEXAFS, XANES, edited by Prins R. and Koningsberger D. C. (Wiley, New York, 1988).
- [19] Joseph B., Iadecola A., Fratini M., Bianconi A., Marcelli A. and Saini N. L., J. Phys.: Condens. Matter 21 432201 (2009).
- [20] Xu W., Marcelli A., Joseph B., Iadecola A., Chu W. S., Di Gioacchino D., Bianconi A., Wu Z. Y. and Saini N. L., J. Phys.: Condens. Matter 22 125701 (2010);
Xu W., Joseph B., Iadecola A., Marcelli A., Chu W. S., Di Gioacchino D., Bianconi A., Wu Z. Y. and Saini N. L., EPL 90 57001 (2010).
- [21] Bondino F., Magnano E., Malvestuto M., Parmigiani F., McGuire M. A., Sefat A. S., Sales B. C., Jin R., Mandrus D., Plummer E. W., Singh D. J. and Mannella N., Phys. Rev. Lett. 101 267001 (2008);
Bondino F., Magnano E., Booth C.H., Offi F., Panaccione G., Malvestuto M., Paolicelli G., Simonelli L., Parmigiani F., McGuire M. A., Sefat A. S., Sales B. C., Jin R., Vilmercati P., Mandrus D., Singh D.J. and Mannella N., Phys. Rev. B 82 014529 (2010).
- [22] Kroll T., Bonhommeau S., Kachel T., Duerr H. A., Werner J., Behr G., Koitzsch A., Huebel R., Leger S., Schoenfelder R., Ariffin A. K., Manzke R., de Groot F. M. F., Fink 4, Eschrig H., Buechner B., and M. Knupfer, Phys. Rev. B 78, 220502 (2008).
- [23] Ignatov A., Zhang C. L., Vannucci M., Croft M., Tyson T. A., Kwok D., Qin Z., Cheong S.-W., arXiv:0808.2134v2.

- [24] Mustre de Leon J., Lezama-Pacheco J., Bianconi A. and Saini N.L., *J. Supercond. Nov. Mag.* 22, 579-583 (2009).
- [25] Chang B. C., You Y. B., Shiu T. J., Tai M. F., Ku H. C., Hsu Y. Y., Jang L. Y., Lee J. F., Wei Z., Ruan K. Q., and Li X. G., *Phys. Rev. B* 80, 165108 (2009).
- [26] Yang W. L., Sorini A. P., Chen C-C., Moritz B., Lee W.-S., Vernay F., Olalde-Velasco P., Denlinger J. D., Delley B., Chu J.-H., Analytis J. G., Fisher I. R., Ren Z. A., Yang J., Lu W., Zhao Z. X., van den Brink J., Hussain Z., Shen Z.-X., and Devereaux T. P., *Phys. Rev. B* 80, 014508 (2009).
- [27] Parks Cheney C., Bondino F., Callcott T. A., Vilmercati P., Ederer D., Magnano E., Malvestuto M., Parmigiani F., Sefat A. S., McGuire M. A., Jin R., Sales B. C., Mandrus D., Singh D. J., Freeland J. W., Mannella N., *Phys. Rev. B* 104518, 81 (2010).
- [28] Mizuguchi Y., Tomioka F., Tsuda S., Yamaguchi T., and Takano Y., *J. Phys. Soc. Jpn.* 78, 074712 (2009).
- [29] Kida, T., Matsunaga, T., Hagiwara, M., Mizuguchi, Y., Takano, Y., Kindo, K., 2009. *J. Phys. Soc. Jpn.* 78, 113701 (2009).
- [30] Bianconi A., Fritsch E., Calas G., and Petiau J., *Phys. Rev. B* 32, 4292 (1985).
- [31] Kvashnina K. O., Butorin S. M., Cui D., Vegelius J., Puranen A., Gens R. and Glatzel P., *J. of Phys: Conf. Ser.* 190, 012191 (2009).
- [32] Chen C. L., Rao S. M., Dong C. L., Chen J. L., Huang T. W, Mok B. H., Ling M. C., Wang W. C., Chang C. L., Chan T. S., Lee J. F., Guo J.-H. and Wu M. K., arXiv:1005.0664v2.